

Modelling structural relaxation in polymeric glasses using the aggregation–fragmentation concept

Aleksey D. Drozdov
Institute for Industrial Mathematics
4 Hanachtom Street
Beersheba, 84311 Israel

Abstract

Governing equations are derived for the kinetics of physical aging in polymeric glasses. An amorphous polymer is treated as an ensemble of cooperatively rearranged regions (CRR). Any CRR is thought of as a string of elementary clusters (EC). Fragmentation of the string may occur at random time at any border between ECs. Two string can aggregate at random time to produce a new string. The processes of aggregation and fragmentation are treated as thermally activated, and the rate of fragmentation is assumed to grow with temperature more rapidly than that for coalescence. This implies that only elementary clusters are stable at the glass transition temperature T_g , whereas below T_g , CRRs containing several ECs remain stable as well. A nonlinear differential equation is developed for the distribution of CRRs with various numbers of ECs. Adjustable parameters of the model are found by fitting experimental data for polycarbonate, poly(methyl methacrylate), polystyrene and poly(vinyl acetate). For all materials, fair agreement is established between observations and results of numerical simulation. For PVAc, the relaxation spectrum found by matching data in a calorimetric test is successfully employed to predict experimental data in a shear relaxation test.

1 Introduction

This paper is concerned with the kinetics of structural relaxation (physical aging) in amorphous glassy polymers. Slow dynamics in out-of-equilibrium disordered media [supercooled liquids, structural (including polymeric) glasses, disordered ferromagnets and antiferromagnets, orientational glasses, vortices in superconductors, dipolar glasses, liquid crystalline colloids, spin glasses, etc.] has attracted substantial attention in the past decade, see, e.g., surveys [1, 2, 3, 4] and the references therein. Unlike most previous studies which focused on equilibrium thermodynamics of glass-like systems [5], the present work deals with the evolution of physical properties of amorphous polymers quenched from some temperature T_0 above the glass transition temperature T_g to a temperature T in the sub- T_g region and isothermally annealed at the temperature T . Changes in the mechanical response, specific volume, configurational entropy and other features of glassy polymers caused by thermal

jumps have been widely studied (both experimentally and theoretically) in the past four decades. We would like to mention here seminal works by Kovacs [6, 7] and Struik [8]. For a detailed review, the reader is referred to [9].

Despite a number of publications concerned with the evolution of internal structure of disordered media after thermal jumps, see [2] for a survey, it is difficult to mention a model (phenomenological or molecular) which correctly predicts experimental data (for example, memory and chaos phenomena in cyclic thermal tests [10, 11]) and establishes an adequate correspondence between observations in various (mechanical, dielectric, calorimetric, dilatometric, etc.) experiments, see, e.g., [12, 13, 14, 15, 16, 17] and the references therein.

An important class of constitutive models for structural relaxation in amorphous materials employs the concept of coarsening in disordered systems [2]. First models belonging to this class (the so-called droplet models) have been proposed a decade ago by Koper and Hilhorst [18] and Fisher and Huse [19] to predict the response of spin glasses. According to their approach, an arbitrary macro-region of a disordered medium is treated as an ensemble of droplets (domains with non-regular boundaries possessing non-zero fractal dimensions) where spins are aligned with one of the ground states. These regions alter with time because of slow coarsening, and the characteristic size of a region grows as a power of time [18] or as a logarithm of time [19]. For a detailed review of phenomenological models for the phase-ordering kinetics, we refer to [20].

Another approach to the description of domain growth has been developed by Ben-Naim and Krapivsky [21, 22, 23, 24]. The present study employs basic ideas of their works to predict enthalpy recovery in amorphous polymers and to study the effect of waiting time t_w on the material response in mechanical (relaxation) tests. We would like to stress two issues that distinguish our constitutive equations from those derived by Ben-Naim and Krapivsky:

1. In the analysis of coalescence, we presume that for any domain, the rate of aggregation with another domain is proportional to the probability density (not to the concentration) of regions with a certain volume (length). This makes solutions of constitutive equations independent of the total number of elementary clusters at the initial instant.
2. We combine the aggregation-fragmentation theory with the concept of internal time. This allows fair approximation of experimental data for the relaxing enthalpy to be established (the conventional approach fails to adequately describe enthalpy recovery during 4 to 5 decades of time).

The concept of internal time is widely used to describe thermo-mechanical response of polymers (for a review, the reader is referred to [25]). In this study, we employ a model with an entropy-driven material clock. This approach was proposed by Struik [8] and was successfully used to predict shear-thickening of polymer solutions in [26].

With reference to the theory of cooperative relaxation [27], an amorphous polymer is thought of as an ensemble of cooperatively rearranging regions (CRR) that relax at random times as they are thermally agitated. A CRR is thought of as a globule consisting of scores of strands of long chains [28]. The characteristic length of a CRR in the vicinity of the glass transition temperature amounts to several nanometers [29].

We introduce a minimal number of strands which permits rearrangement, ν , and suppose that the number of strands in any CRR reads $n\nu$, where n is an integer and ν is the number

of strands in an elementary cluster (EC). The concept of elementary domains was first introduced by Adam and Gibbs [27] for amorphous polymers and by Kadanoff [30] for spin glasses. For a discussion of the Kadanoff conjecture (near the critical point, large blocks of spins behave like individual spins) see [31, 32]. Description of the aging process in glassy polymers in terms of models with finite numbers of states was suggested by Chow [33] and Robertson [34, 35].

Unlike previous studies where the domain growth was interpreted as random motion of their boundaries annihilated at the contact points, see, e.g., [24], we treat structural recovery as a result of two (thermally activated) processes with different dependences of their rates on temperature: fragmentation of large regions and aggregation of small ones. An indirect confirmation of this picture is provided by experimental data in calorimetric tests at various temperatures T_k in the sub- T_g region. Observations reveal that if $T_2 > T_1$, the relaxing enthalpy ΔH in a test with the temperature T_1 exceeds that in a test with the temperature T_2 at small times, and the inverse is true at large times.

The exposition is organized as follows. In Section 2, constitutive equations are derived for enthalpy recovery in amorphous glassy polymers. These equations are verified in Section 3 by comparison with experimental data for polycarbonate, polystyrene, poly(methyl methacrylate) and poly(vinyl acetate). The purpose of fitting observations is two-fold: (i) to confirm that the model can correctly predict measurements, and (ii) to analyze the effect of temperature T on material parameters. In Section 4, the model is subject to a more elaborate evaluation: after determining adjustable parameters by matching data in calorimetric tests, we use the probability density of CRRs with various energies to fit the material response in a static mechanical test. To make this possible, a model is derived for stress relaxation in disordered media based on the traps concept (for detail, we refer to [36, 37]). Some concluding remarks are formulated in Section 5.

2 Constitutive equations for domain growth

The following hypotheses are introduced to develop a master equation for the concentration of CRRs:

1. Structural relaxation in a disordered medium is governed by two processes at the micro-level: fragmentation of CRRs and their aggregation.
2. Denote by $P(t, n)$ the number of CRRs (per unit mass) at time t consisting of $n + 1$ elementary clusters. The quantity $P(t, n)$ is the mass concentration of CRRs containing n borders between ECs subject to fragmentation (to simplify the analysis, any CRR is thought of as a linear “string” of ECs). The function $P(t, n)$ obeys the conservation law

$$\sum_{n=0}^{\infty} (n + 1) P(t, n) = \Xi_0, \quad (1)$$

where Ξ_0 is the number of ECs per unit mass.

3. The fragmentation process is characterized by its rate γ that equals the number of fragmentation acts per boundary between ECs per unit time. We assume γ to be a

function of the current temperature T only. The rate of changes in the quantity $P(t, n)$ induced by fragmentation is given by

$$V_f(t, n) = \gamma \left[-nP(t, n) + 2 \sum_{m=n+1}^{\infty} P(t, m) \right]. \quad (2)$$

The first term on the right-hand side of Eq. (2) determines the number of CRRs (containing n boundaries) destroyed by fragmentation, whereas the other term is the rate of creation of CRRs with n boundaries caused by fragmentation of relaxing regions containing larger number of elementary clusters. The physical meaning of formula (2) is discussed in detail in [38].

4. Coalescence of relaxing regions occurs when CRRs (with n and m borders between ECs) merge and create a new CRR (with $n + m + 1$ borders). The rate of aggregation of an individual CRR with n boundaries between ECs with CRRs with m borders is proportional to the density of CRRs with m boundaries (the ratio $\varphi(t, m)$ of the number of CRRs with m boundaries to the total number of CRRs per unit mass) and to the number of random meetings, $\Gamma_{n,m}$, for two CRRs with n and m boundaries. The rate of changes in the quantity $P(t, n)$ induced by coalescence reads

$$\begin{aligned} V_c(t, n) = & -P(t, n) \left[\sum_{m=0, m \neq n}^{\infty} \Gamma_{n,m} \varphi(t, m) + 2\Gamma_{n,n} \varphi(t, n) \right] \\ & + \sum_{m=0}^{n-1} \Gamma_{m, n-m-1} P(t, m) \varphi(t, n-m-1) \end{aligned} \quad (3)$$

with

$$\varphi(t, n) = \frac{P(t, n)}{\sum_{m=0}^{\infty} P(t, m)}. \quad (4)$$

The first two terms on the right-hand side of Eq. (3) determine the number of CRRs destroyed by aggregation with other CRRs (the coefficient 2 in the second term means that two relaxing regions with n borders disappear when they meet one another). The last term in Eq. (3) characterizes the rate of creation of CRRs with n boundaries by aggregation of two relaxing regions with smaller numbers of ECs.

5. The rate $\Gamma_{n,m}$ by which regions with n and m boundaries aggregate decays exponentially with the growth of the indices n and m ,

$$\Gamma_{n,m} = L\gamma \exp[-\lambda(n+m)], \quad (5)$$

where L and λ are material parameters. Assumption (5) is conventional for the treatment of (short-range) interactions between CRRs, but it differs from standard relations based on the theory of anomalous diffusion, see, e.g., [39] and the references therein, which lead to the power law dependence of $\Gamma_{m,n}$ on n and m . Our numerical analysis shows that replacement of Eq. (5) by a power law does not affect significantly the accuracy of fitting.

6. We employ the concept of material (reduced) time and suppose that γ is the rate with respect to some internal time τ . The rate of fragmentation with respect to the “universal” time t reads

$$\gamma_0 = a\gamma, \quad (6)$$

where a is a shift factor.

7. For polymers with an entropy-driven material clock [8], we set

$$\ln a = -\kappa_0 s, \quad (7)$$

where κ_0 is some material parameter and s is the configurational entropy per EC.

8. The configurational entropy s is defined by the Boltzmann’s formula

$$s(t) = -k_B \sum_{n=0}^{\infty} \varphi(t, n) \ln \varphi(t, n), \quad (8)$$

where k_B is Boltzmann’s constant. It is worth noting some difference between Eq. (8) and conventional relations, see, e.g., [40]. In Eq. (8) the configurational entropy s is defined per elementary cluster, whereas traditional formulas define configurational entropy per CRR.

It follows from Eqs. (2) to (7) that the current concentration of CRRs (per unit mass) is governed by the differential equation

$$\begin{aligned} \frac{\partial P}{\partial t}(t, n) = & \gamma_0 \exp(-\kappa s(t)) \left\{ -nP(t, n) + 2 \sum_{m=n+1}^{\infty} P(t, m) - \frac{L}{\sum_{m=0}^{\infty} P(t, m)} \right. \\ & \times \left[P(t, n) \sum_{m=0, m \neq n}^{\infty} P(t, m) \exp(-\lambda(n+m)) + 2P^2(t, n) \exp(-2\lambda n) \right. \\ & \left. \left. - \exp(-\lambda(n-1)) \sum_{m=0}^{n-1} P(t, m) P(t, n-m-1) \right] \right\}, \end{aligned} \quad (9)$$

where $\kappa = k_B \kappa_0$.

The study is confined to one-step “quench-and-wait” tests, when a polymer equilibrated at some temperature $T_0 > T_g$ is quenched to a temperature $T < T_g$ and is annealed at the temperature T ,

$$T(t) = \begin{cases} T_0, & t < 0, \\ T, & t > 0. \end{cases} \quad (10)$$

Assuming that above the glass transition temperature T_g , only elementary clusters may exist, we postulate

$$P(0, n) = \Xi_0 \delta_{n,0}, \quad (11)$$

where $\delta_{n,m}$ is the Kronecker delta. The solution $P(t, n)$ of Eqs. (8), (9) and (11) is independent of the total number of ECs, Ξ_0 , and it is determined by 4 adjustable parameters: L , γ_0 , κ and λ .

Let $h(t)$ be the configurational enthalpy per EC. Assuming h to be expressed in terms of the configurational entropy s by the conventional relationship,

$$\frac{\partial h}{\partial s} = T,$$

and integrating this equality for the thermal program (10), we find that

$$h(t) = Ts(t) \quad (t > 0). \quad (12)$$

Multiplying Eq. (12) by the concentration of ECs, Ξ_0 , we calculate the configurational enthalpy per unit mass. Assuming the relaxing enthalpy ΔH (measured in calorimetric tests) to coincide with the configurational enthalpy, we arrive at the formula

$$\Delta H(t) = -\Lambda \sum_{n=0}^{\infty} \varphi(t, n) \ln \varphi(t, n) \quad (13)$$

with

$$\Lambda = k_B T \Xi_0. \quad (14)$$

3 Comparison with observations in calorimetric tests

We begin with experimental data for polycarbonate. For a detailed description of samples and the experimental procedure, see [41]. Adjustable parameters are found by matching observations using the steepest-descent procedure. Figure 1 demonstrates that the model correctly predicts experimental data at two temperatures in the sub- T_g region. Setting $T = T_g = 420$ K in Eq. (14), using mass density $\rho = 1.196$ g/cm³ [42], and the value $\Lambda = 0.8$ J/g found by fitting observations, we obtain

$$\Xi_0 = 1.15 \cdot 10^{26} \text{ m}^{-3}. \quad (15)$$

This value is in accord with $\Xi_0 = 3.6 \cdot 10^{26} \text{ m}^{-3}$ for polytetrafluoroethylene [43], but it is less than concentrations of holes measured for a series of polycarbonates using positron lifetime spectroscopy [44] (for comparison, we assume that any EC may be associated with a micro-hole). To explain this discrepancy, we recall that (i) Bohlen et al. [44] presumed a Gaussian distribution of holes with a peak far above the zero volume, whereas our calculations demonstrate that the probability density of CRRs substantially differs from the Gaussian ansatz (see Figure 2), and (ii) the value (15) is for temperatures in the vicinity of T_g , while the PALS measurements were carried out at room temperature.

Suppose that the effect of temperature on the rate of fragmentation γ_0 is described by the Arrhenius formula

$$\gamma_0(T) = \gamma_* \exp\left(-\frac{\Delta E}{RT}\right), \quad (16)$$

where ΔE is some activation energy and R is the universal gas constant. Applying Eq. (16) to two temperatures, T_1 and T_2 , in the sub- T_g region, we find that

$$\Delta E = \frac{RT_g^2}{T_2 - T_1} \ln \frac{\gamma_0(T_2)}{\gamma_0(T_1)}. \quad (17)$$

Taking values of $\gamma_0(T_k)$ determined by fitting experimental data (Figure 1), we obtain $\Delta E = 174.1$ kcal/mol, which is in fair agreement with $\Delta E = 173.6$ kcal/mol found by shift of relaxation curves measured at various temperatures in the vicinity of the glass transition temperature [25].

According to Figure 1, an increase in temperature T leads to a sharp decrease in the relative rate of aggregation L and to an increase in the parameter λ . This conclusion is in fair agreement with our hypothesis that above the glass transition temperature T_g only elementary clusters exist (because the rate of merging vanishes, the growth of CRRs caused by their coalescence is prohibited). It is worth noting that an increase in λ with temperature observed in experiments makes questionable models of aggregation that are based on the diffusion mechanism, see [39], provided that the coefficient λ in Eq. (5) may be associated (at least, to some extent) with the decrease in the diffusion coefficient induced by the growth of mass of domains to be aggregated.

The equilibrium distributions depicted in Figure 2 are characterized by their mean value M_1 and variance M_2 ,

$$M_1 = \sum_{n=0}^{\infty} n\varphi(\infty, n), \quad M_2 = \sum_{n=0}^{\infty} (n - M_1)^2 \varphi(\infty, n). \quad (18)$$

Numerical simulation demonstrates that the quantities M_1 and M_2 substantially increase with a decrease in T . This is in accord with the conventional approach to the description of structural relaxation [2, 5] which presumes a substantial growth in the roughness of the energy landscape with a decrease in temperature (which, in turn, results in a monotonic increase in the variance of the distribution of CRRs with $\Delta T = T_g - T$).

We proceed with matching experimental data for polystyrene using the above algorithm. For a description of the experimental procedure, we refer to [45]. Figure 3 reveals fair agreement between observations at two temperatures in the sub- T_g region and results of numerical analysis. Equation (14) with $T = T_g = 373.0$ K, $\rho = 1.04$ g/cm³ and $\Lambda = 1.1$ J/g results in $\Xi_0 = 2.55 \cdot 10^{26}$ m⁻³, which is in acceptable agreement with PALS measurements. It follows from Eq. (17) and Figure 3 that the activation energy $\Delta E = 136.4$ kcal/mol, which is rather close to the value $\Delta E = 170.5$ kcal/mol found by shift of creep curves in the sub- T_g region [46]. The equilibrium distributions of CRRs containing various numbers of elementary clusters are plotted in Figure 4 which demonstrate that an increase in ΔT leads to an increase in M_1 and M_2 . This is in qualitative agreement with conventional models for aging that predict the growth of roughness of the energy landscape with a decrease in temperature.

Experimental data for polycarbonate and polystyrene (only at two temperatures in the sub- T_g region) are not sufficient to analyze the effect of temperature on the kinetics of structural relaxation. To study changes in adjustable parameters caused by the annealing temperature T , we match observations for poly(methyl methacrylate). For a detailed description of samples and the experimental procedure, we refer to [47]. We begin approximation with measurements at the lowest temperature $T = 375.0$ K and determine parameters L , γ_0 , κ , λ and Λ using a version of the steepest-descent algorithm. Afterwards, we fix Λ (an analog of the number of elementary clusters per unit mass) and fit data at other temperatures using 4 constants: L , γ_0 , κ and λ . The assumption that the parameter κ is temperature-dependent differs the treatment of data for poly(methyl methacrylate) from that for polycarbonate and

polystyrene (for which κ was assumed to be independent of temperature). This is done to ensure better quality of matching experimental data. Figures 5 to 10 demonstrate fair agreement between observations and results of numerical simulation.

The rate of fragmentation γ_0 is plotted versus the increment of temperature ΔT in Figure 11. This figure shows that experimental data are correctly approximated by the “linear” function

$$\log \gamma_0 = a_0 - a_1 \Delta T \quad (19)$$

with adjustable parameters a_k . Equations (16) and (19) imply that in the vicinity of the glass transition temperature T_g , the activation energy ΔE is given by

$$\Delta E = a_1 R T_g^2 \ln 10.$$

It follows from this formula and Figure 11 that $\Delta E = 70.81$ kcal/mol, which is in excellent agreement with data for activation energy obtained by shift of creep and relaxation curves at various temperatures. For example, using WLF parameters for poly(methyl methacrylate) [48], we arrive at the value $\Delta E = 83.2$ kcal/mol, which is close to our result. This is in contrast with the Cowie–Ferguson model [47] which results in the value $\Delta E = 164.8$ kcal/mol for the same set of experimental data.

The parameter L (which characterizes the ratio of the rate of aggregation to the rate of fragmentation) is depicted in Figure 11 versus the increment of temperature ΔT . Experimental data are fairly well approximated by the linear function

$$L = b_0 + b_1 \Delta T \quad (20)$$

with adjustable parameters b_k . Equation (20) implies that L monotonically increases with a decrease in temperature T , which means that the rate of aggregation of elementary clusters grows with a departure from the glass transition temperature.

The dimensionless parameters λ and κ are plotted versus the increment of temperature ΔT in Figure 12. Experimental data are approximated by the functions

$$\lambda = c_0 - c_1 \Delta T, \quad \log \kappa = C_0 - C_1 \Delta T, \quad (21)$$

where c_k and C_k are adjustable parameters. Figure 12 demonstrates that the quantities λ and κ increase with temperature. Far below the glass transition point (about 30 K below T_g) the parameter λ vanishes, which results in an essential simplification of Eq. (9) (whose coefficients become independent of n and m , which allows a method of generating functions to be applied to develop analytical solutions [49]). Explicit solutions to the governing equations are, however, beyond the scope of the present study.

It is worth noting that phenomenological models for physical aging in polymers presume that the effects of temperature and structure may be separated, see, e.g., [7]. Results of numerical simulation reveal that this hypothesis is valid when the increment of temperature ΔT is not too small (say, it exceeds 15 K) which implies that κ becomes weakly dependent on temperature.

Conventional constitutive equations for structural relaxation in amorphous polymers employ the random energy model [50], according to which the distribution of relaxing regions with various energies is Gaussian with temperature-dependent mean value and standard

deviation. Fitting experimental data obtained in mechanical tests for a number of glassy polymers show that the standard deviation of energy of CRRs, Σ , linearly decreases with temperature and vanishes at some critical temperature T_{cr} slightly above T_g [37]. Because the present study is based on the assumption that only elementary clusters are stable at the glass transition temperature (which implies that $T_{\text{cr}} = T_g$), our purpose now is to demonstrate that

$$\Sigma = \sqrt{M_2}$$

linearly increases with ΔT in the sub- T_g region. Figure 13 shows that with an acceptable level of accuracy the graphs $M_1(\Delta T)$ and $\Sigma(\Delta T)$ are linear. Approximation of experimental data by the functions

$$M_1 = m_1 \Delta T, \quad \Sigma = m_2 \Delta T \quad (22)$$

yields $m_2 = 0.15 \text{ K}^{-1}$. This result is in good agreement with $m_2 = 0.09 \text{ K}^{-1}$ for polycarbonate and $m_2 = 0.53 \text{ K}^{-1}$ for poly(vinyl acetate) found by fitting observations in static and dynamic mechanical tests [37].

Hitherto, only average characteristics (first moments and entropy) of the distribution of CRRs have been compared with observations. To reveal that the distribution of relaxing regions $\varphi(t, n)$ itself is in agreement with measurements, we analyze experimental data for poly(vinyl acetate) in calorimetric and mechanical (relaxation) tests. For a description of the experimental procedure, see [16].

We begin with matching observations in a calorimetric test at $T = 303 \text{ K}$. Figure 14 demonstrates fair correspondence between experimental data and results of numerical simulation. Setting $T = T_g = 315 \text{ K}$ in Eq. (14) and using the values $\rho = 1.182 \text{ g/cm}^3$ [51] and $\Lambda = 1.6 \text{ J/g}$ (Figure 14), we arrive at $\Xi_0 = 3.24 \cdot 10^{26} \text{ m}^{-3}$, which is in good accord with the concentration of holes measured by PALS for polytetrafluoroethylene [43]. All adjustable parameters for PVAc (except for the rate of fragmentation γ_0) are similar to those for PC, PS and PMMA. The quantity γ_0 is smaller than that for other polymers. This may be explained by the differences in the glass transition temperatures of materials under consideration (glass transition points for PC, PS and PMMA substantially exceed T_g for PVAc) and the fact that fragmentation and aggregation of CRRs are thermally activated.

To fit data in mechanical tests, stress-strain relations should be derived for amorphous glassy polymers under short-term mechanical loading (compared to the waiting time t_w). In this work, we briefly sketch the development of constitutive equations confining ourselves to uniaxial relaxation tests. Greater detail of derivations can be found in [37].

4 The mechanical response in relaxation tests

In accord with the hoping concept, see, e.g., [28], a relaxing region is treated as a point located at the bottom level of its potential well on the energy landscape. Rearrangement of CRRs is modeled as hops of relaxing regions to higher energy levels. Hops occur at random times, and they are driven by thermal fluctuations. Below the glass transition temperature, energy barriers between potential wells are assumed to be so high that thermally agitated CRRs cannot leave their traps. Adopting the transition-state theory [52], we suppose that rearrangements occur when CRRs reach some liquid-like (reference) energy level. The posi-

tion of this level is not fixed, but it slowly ascends in time approaching some limiting value as $t_w \rightarrow \infty$.

Any potential well is described by its depth $w > 0$ with respect to the position of the reference energy level at the initial instant (immediately after the quench). Following our treatment of CRRs as aggregates composed of integer numbers of elementary clusters, we assume that the set of available energies w is countable,

$$w = w_1, w_2, \dots, w_n, \dots,$$

and the value w_n is proportional to the volume (length) of an appropriate CRR (string),

$$w_n = \alpha n, \quad (23)$$

where $\alpha > 0$ is an adjustable parameter.

Let $q(\omega)d\omega$ be the probability for a CRR to reach (in a hop) the energy level that exceeds its bottom level by an energy ω' located in the interval $[\omega, \omega + d\omega]$. Referring to the extreme value statistics [2], we set

$$q(\omega) = A \exp(-A\omega),$$

where A is a material constant. The probability to reach the reference state in a hop for a CRR trapped in a potential well with the depth w reads

$$Q(t_w, w) = \int_{w+\Omega(t_w)}^{\infty} q(\omega)d\omega = \exp[-A(w + \Omega(t_w))].$$

Here $\Omega(t_w)$ is the increment of the reference energy level after the waiting time t_w with respect to that at the initial instant, and we take into account that the duration of conventional mechanical tests is negligible compared to t_w .

The rate of hops in a potential well, Γ , is defined as the number of hops (of an arbitrary intensity) per unit time. Assuming Γ to be independent of w (according to the theory of thermally activated processes, Γ is a function of the current temperature T only), and multiplying the rate of hops Γ by the probability of reaching the liquid-like state in a hop $Q(t_w, w)$, we arrive at the Eyring formula for the rate of rearrangement [53],

$$R(t_w, w) = \Gamma_0(t_w) \exp(-Aw), \quad \Gamma_0 = \Gamma \exp(A\Omega(t_w)). \quad (24)$$

The rate of rearrangement, $R(t_w, w)$, can be thought of as the ratio of the number of rearranging regions (per unit time) to the number of CRRs to be rearranged,

$$R(t_w, w) = -\frac{1}{\Xi(t, t_w, w)} \frac{\partial \Xi}{\partial t}(t, t_w, w). \quad (25)$$

For relaxation tests, the quantity $\Xi(t, t_w, w)$ is the number of CRRs (per unit mass) located in cages with energy w that have not been rearranged until time t (which is measured from the beginning of the test). Integration of Eq. (25) implies that

$$\Xi(t, t_w, w) = \Xi(0, t_w, w) \exp[-R(t_w, w)t]. \quad (26)$$

The initial condition for Eq. (26) is given by

$$\Xi(0, t_w, w_n) = N(t_w) \varphi(t_e, n), \quad (27)$$

where

$$N(t_w) = \sum_{n=0}^{\infty} P(t_w, n)$$

is the number of CRRs (per unit mass) after annealing for the time t_w .

The natural configuration of a CRR after rearrangement is assumed to coincide with the deformed configuration of the viscoelastic medium at the instant of rearrangement. This implies that rearranged CRRs are stress-free in a relaxation test, and only non-rearranged regions have non-zero mechanical energies. The strain energy density of an amorphous polymer (per unit mass) under uniaxial loading, U , equals the sum of mechanical energies of individual regions. A CRR is thought of as a linear elastic medium with the potential energy of deformation

$$\frac{1}{2} \mu \epsilon^2,$$

where μ is the rigidity and ϵ is the macro-strain (for definiteness, shear deformation is considered). Combining this expression with Eqs. (23), (24), (26) and (27), we find that

$$\begin{aligned} U(t, t_w) &= \frac{1}{2} \mu \epsilon^2 \sum_{n=1}^{\infty} \Xi(t, t_w, w_n) \\ &= \frac{1}{2} \mu N(t_w) \epsilon^2 \sum_{n=1}^{\infty} \varphi(t_w, n) \exp[-\Gamma_0(t_w) \exp(-\alpha_0 n) t], \end{aligned} \quad (28)$$

where $\alpha_0 = \alpha A$. The stress σ is expressed in terms of the mechanical energy U by the formula

$$\sigma = \rho \frac{\partial U}{\partial \epsilon}.$$

This equality together with Eq. (28) implies that

$$G(t, t_w) = G_0(t_w) \sum_{n=1}^{\infty} \varphi(t_w, n) \exp[-\Gamma_0(t_w) \exp(-\alpha_0 n) t], \quad (29)$$

where $G(t, t_w) = \sigma(t)/\epsilon$ is the current shear modulus, $G_0(t_w) = \mu N(t_w)$ is the initial modulus.

To verify the model, we calculate the distribution of CRRs, $\varphi(t_w, n)$, using Eqs. (8), (9) and (11) with adjustable parameters found by fitting observations in the calorimetric test, and match experimental data in the relaxation test by Eq. (29). Given a constant G_0 , the material parameters Γ_0 and α_0 are calculated using the steepest-descent procedure. The initial shear modulus G_0 is determined by the least-square algorithm. Figure 15 demonstrates fair agreement between observations and results of numerical simulation.

It is worth noting that our constitutive equations employ two independent time-scales for the description of structural recovery in polymeric glasses. One scale is entirely determined by the distribution function $\varphi(t_w, n)$. The other time-scale characterizes the ascent of the liquid-like energy level with respect to the energy landscape, and it is portrayed by the function $\Omega(t_w)$. This approach is in agreement with that recently proposed by Tanaka [54], where two order parameters were used to predict slow dynamics in supercooled liquids.

5 Conclusions

A model is derived for structural relaxation in amorphous glassy polymers after thermal jumps. A polymeric glass is treated as an ensemble of cooperatively rearranging regions whose concentration changes with time because of their fragmentation and aggregation. A CRR is modeled as a string (linear chain) of elementary clusters. Fragmentation of the string may occur at random time at any border between elementary clusters with equal probability. Aggregation of relaxing regions occurs at random time as well. The rate of coalescence for two CRRs decreases exponentially with the growth of their sizes. With a decrease in temperature T , the rates of fragmentation and aggregation decrease, but the rate of fragmentation reduces more rapidly. This implies that only elementary clusters exist at the glass transition temperature T_g , whereas in the sub- T_g region, CRRs consisting of several ECs may be stable as well.

To verify constitutive equations, we fit experimental data for relaxing enthalpy for polycarbonate, polystyrene, poly(methyl methacrylate) and poly(vinyl acetate). Fair agreement is demonstrated between observations in calorimetric tests and results of numerical analysis. Material parameters found by fitting measurements are in good accord with those determined experimentally in other tests.

To establish correspondence between observations in calorimetric and mechanical tests, we find material parameters for PVAc by fitting relaxing enthalpy, determine the relaxation spectrum and use this spectrum to match data in mechanical (static) test. An acceptable agreement between experimental data for the shear modulus and numerical predictions confirms our belief that the model may be employed for the analysis of physical aging in tests, where several experimental methods are applied simultaneously.

Acknowledgement

The work was supported by the Israeli Ministry of Science through grant 1202-1-98.

References

- [1] Ediger, M.D.; Angell, C.A.; Nagel, S.R. J Phys Chem 1996, 100, 13200.
- [2] Bouchaud, J.-P.; Cugliandolo, L.F.; Kurchan, J.; Mezard, M. In Spin Glasses and Random Fields; Young, A.P., Ed.; World Scientific: Singapore, 1998; p. 161.
- [3] Kob, W. Preprint cond-mat/9911023.
- [4] Hammann, J.; Vincent, E.; Dupuis, V.; Alba, M.; Ocio, M.; Bouchaud, J.-P. Preprint cond-mat/9911269.
- [5] Mezard, M.; Parisi, G. Preprint cond-mat/0002128.
- [6] Kovacs, A.J. Adv Polym Sci 1964, 3, 394.
- [7] Kovacs, A.J.; Aklonis, J.J.; Hutchinson, J.M.; Ramos, A.R. J Polym Sci: Polym Phys Ed 1979, 17, 1097.
- [8] Struik, L.C.E. Physical Ageing in Amorphous Polymers and Other Materials; Elsevier: Amsterdam, 1978.
- [9] McKenna, G.B. In Comprehensive Polymer Science; Booth, C.; Price, C., Eds.; Pergamon Press: Oxford, 1989; Vol. 2, p. 311.
- [10] Bellon, L.; Ciliberto, S.; Laroche, C. Preprint cond-mat/9905160.
- [11] Bellon, L.; Ciliberto, S.; Laroche, C. Preprint cond-mat/9906162.
- [12] Delin, M.; Rychwalski, R.W.; Kubat, J.; Klason, C.; Hutchinson, J.M. Polym Eng Sci 1996, 36, 2955.
- [13] Davis, W.J.; Pethrick, R.A. Polymer 1998, 39, 255.
- [14] Shelby, M.D.; Wilkes, G.L. Polymer 1998, 39, 6767.
- [15] Cowie, J.M.G.; Harris, S.; McEwen, I.J. Macromolecules 1998, 31, 2611.
- [16] Cowie, J.M.G.; Ferguson, R.; Harris, S.; McEwen, I.J. Polymer 1998, 39, 4393.
- [17] Hutchinson, J.M.; Smith, S.; Horne, B.; Gourlay, G.M. Macromolecules 1999, 32, 5046.
- [18] Koper, G.J.M.; Hilhorst, H.J. J Phys (France) 1988, 49, 429.
- [19] Fisher, D.S.; Huse, D.A. Phys Rev B 1988, 38, 386.
- [20] Bray, A.J. Adv Phys 1994, 43, 357.
- [21] Ben-Naim, E.; Krapivsky, P.L. Phys Rev E 1995, 52, 6066.
- [22] Ben-Naim, E.; Krapivsky, P.L. Phys Rev E 1996, 54, 3562.

- [23] Ben-Naim, E.; Krapivsky, P.L. *Phys Rev E* 1997, 56, 3788.
- [24] Ben-Naim, E.; Krapivsky, P.L. *J Stat Phys* 1998, 93, 583.
- [25] Drozdov, A.D. *Mechanics of Viscoelastic Solids*; Wiley: Chichester, 1998.
- [26] Drozdov, A.D. *Mathl Comput Modelling* 1997, 25, 45.
- [27] Adam, G.; Gibbs, J.H. *J Chem Phys* 1965, 43, 139.
- [28] Sollich, P. *Phys Rev E* 1998, 58, 738.
- [29] Rizos, A.K.; Ngai, K.L. *Phys Rev E* 1999, 59, 612.
- [30] Kadanoff, L.P. *Physics* 1966, 2, 263.
- [31] Levitan, B.; Domany, E. *J Stat Phys* 1998, 93, 501.
- [32] Baker, G.A. *J Stat Phys* 1998, 93, 573.
- [33] Chow, T.S. *J Chem Phys* 1983, 79, 4602.
- [34] Robertson, R.E. *J Appl Phys* 1978, 49, 5048.
- [35] Robertson, R.E.; Simha, R.; Curro, J.G. *Macromolecules* 1984, 17, 911.
- [36] Drozdov, A.D. *Modelling Simul Mater Sci Eng* 1999, 7, 1045.
- [37] Drozdov, A.D. *Europhys Lett* 2000, 49, 569.
- [38] Redner, S. In *Statistical Models for the Fracture of Disorder Media*; Herrmann, H.J.; Roux, S., Eds.; North-Holland: Amsterdam, 1990; Chapter 10.
- [39] Kuczka, J.; Hänggi, P.; Gadowski, A. *Phys Rev E* 1995, 51, 5762.
- [40] Avramov, I.; Milchev, A. *J Non-Cryst Solids* 1988, 104, 253.
- [41] Bauwens-Crowet, C.; Bauwens, J.-C. *Polymer* 1987, 28, 1863.
- [42] Hill, A.J.; Katz, I.M.; Jones, P.L. *Polym Eng Sci* 1990, 30, 762.
- [43] Dlubek, G.; Saarinen, K.; Fretwell, H.M. *J Polym Sci B: Polym Phys* 1998, 36, 1513.
- [44] Bohlen, J.; Wolff, J.; Kirchheim, R. *Macromolecules* 1999, 32, 3766.
- [45] Roe, R.-J.; Millman, G.M. *Polym Eng Sci* 1983, 23, 318.
- [46] Schwarzl, F.R.; Zahradnik, F. *Rheol Acta* 1980, 19, 137.
- [47] Cowie, J.M.G.; Ferguson, R. *Polymer* 1993, 34, 2135.
- [48] Aklonis, J.J.; MacKnight, W.J.; Shen, M. *Introduction to Polymer Viscoelasticity*; Wiley-Interscience: New York, 1972.

- [49] Krapivsky, P.L.; Ben-Naim, E. Preprint cond-mat/0003390.
- [50] Richert, R.; Bässler, H. J Phys: Condens Matter 1990, 2, 2273.
- [51] Kubat, M.J.; Vernel, J.; Rychwalski, R.W.; Kubat, J. Polym Eng Sci 1998, 38, 1261.
- [52] Goldstein, M. J Chem Phys 1969, 51, 3728.
- [53] Eyring, H. J Chem Phys 1936, 4, 283.
- [54] Tanaka, H. J Phys: Condens Matter 1999, 11, L159.

List of figures

Figure 1: The relaxation enthalpy ΔH J/g versus time t h for polycarbonate annealed at the temperature T K. Circles: experimental data [41]. Solid lines: numerical simulation with $\Lambda = 0.8$ J/g and $\kappa = 1.0$. Curve 1: $T = 408.0$, $L = 80.0$, $\lambda = 0.3$, $\gamma_0 = 10^3$ h⁻¹; curve 2: $T = 413.0$, $L = 5.0$, $\lambda = 1.2$, $\gamma_0 = 1.2 \cdot 10^4$ h⁻¹

Figure 2: The equilibrium distribution of CRRs $\varphi = \varphi(\infty, n)$ for polycarbonate. Unfilled circles: $T = 408$ K, $M_1 = 4.9328$, $M_2 = 9.8743$. Filled circles: $T = 413$ K, $M_1 = 0.9157$, $M_2 = 0.6758$

Figure 3: The relaxation enthalpy ΔH J/g versus time t h for polystyrene annealed at the temperature T K. Circles: experimental data [45]. Solid lines: numerical simulation with $\Lambda = 1.1$ J/g and $\kappa = 1.0$. Curve 1: $T = 363.0$, $L = 80.0$, $\lambda = 0.3$, $\gamma_0 = 10^3$ h⁻¹; curve 2: $T = 366.0$, $L = 35.0$, $\lambda = 0.5$, $\gamma_0 = 4.4 \cdot 10^3$ h⁻¹

Figure 4: The equilibrium distribution of CRRs $\varphi = \varphi(\infty, n)$ for polystyrene. Unfilled circles: $T = 363$ K, $M_1 = 4.9328$, $M_2 = 9.8743$. Filled circles: $T = 366$ K, $M_1 = 2.7906$, $M_2 = 3.6336$. The relaxation enthalpy ΔH J/g versus time t h for poly(methyl methacrylate) at $T = 375.0$ K (unfilled circles: experimental data [47]; solid line: numerical simulation) and the final distribution of CRRs $\varphi = \varphi(t_w, n)$ with $t_w = 10^{2.5}$ h

Figure 5: The relaxation enthalpy ΔH J/g versus time t h for poly(methyl methacrylate) at $T = 375.0$ K (unfilled circles: experimental data [47]; solid line: numerical simulation) and the final distribution of CRRs $\varphi = \varphi(t_w, n)$ with $t_w = 10^{2.5}$ h

Figure 6: The relaxation enthalpy ΔH J/g versus time t h for poly(methyl methacrylate) at $T = 377.5$ K (unfilled circles: experimental data [47]; solid line: numerical simulation) and the final distribution of CRRs $\varphi = \varphi(t_w, n)$ with $t_w = 10^{2.5}$ h

Figure 7: The relaxation enthalpy ΔH J/g versus time t h for poly(methyl methacrylate) at $T = 380.0$ K (unfilled circles: experimental data [47]; solid line: numerical simulation) and the final distribution of CRRs $\varphi = \varphi(t_w, n)$ with $t_w = 10^{2.5}$ h

Figure 8: The relaxation enthalpy ΔH J/g versus time t h for poly(methyl methacrylate) at $T = 382.5$ K (unfilled circles: experimental data [47]; solid line: numerical simulation) and the final distribution of CRRs $\varphi = \varphi(t_w, n)$ with $t_w = 10^{2.5}$ h

Figure 9: The relaxation enthalpy ΔH J/g versus time t h for poly(methyl methacrylate) at $T = 385.0$ K (unfilled circles: experimental data [47]; solid line: numerical simulation) and the final distribution of CRRs $\varphi = \varphi(t_w, n)$ with $t_w = 10^{2.5}$ h

Figure 10: The relaxation enthalpy ΔH J/g versus time t h for poly(methyl methacrylate) at $T = 387.5$ K (unfilled circles: experimental data [47]; solid line: numerical simulation) and the final distribution of CRRs $\varphi = \varphi(t_w, n)$ with $t_w = 10^{2.5}$ h

Figure 11: The rate of fragmentation γ_0 h⁻¹ (unfilled circles) and the dimensionless parameter L (filled circles) versus the increment of temperature ΔT K for poly(methyl methacrylate). Symbols: treatment of observations [47]. Solid lines: approximation of the experimental data by Eqs. (19) and (20) with $a_0 = 4.3733$, $a_1 = 0.0993$ and $b_0 = 3.8507$ and

$$b_1 = 1.2686$$

Figure 12: The dimensionless parameters λ (unfilled circles) and κ (filled circles) versus the increment of temperature ΔT K for poly(methyl methacrylate). Symbols: treatment of observations [47]. Solid lines: approximation of the experimental data by Eq. (21) with $c_0 = 0.7611$, $c_1 = 0.0274$ and $C_0 = 0.7173$, $C_1 = 0.0310$

Figure 13: The average number of borders between ECs in a CRR, M_1 , and its standard deviation, $\Sigma = M_2^{\frac{1}{2}}$, versus the increment of temperature ΔT K for poly(methyl methacrylate). Circles: treatment of observations [47]. Solid lines: approximation of the experimental data by Eq. (22) with $m_1 = 0.2037$ and $m_2 = 0.1533$. Curve 1: M_1 ; curve 2: Σ

Figure 14: The relaxation enthalpy ΔH J/g versus time t h for poly(vinyl acetate) annealed at $T = 303$ K. Unfilled circles: experimental data [16]. Solid line: numerical simulation with $\Lambda = 1.6$ J/g, $\kappa = 2.9$, $L = 20.0$, $\lambda = 0.45$, $\gamma_0 = 4.74 \cdot 10^2 \text{ h}^{-1}$. Filled circles: the distribution of CRRs $\varphi = \varphi(t_w, n)$ with $t_w = 10^{2.5}$ h, $M_1 = 2.4209$, $M_2 = 3.2730$

Figure 15: The shear modulus G GPa versus time t s for poly(vinyl acetate) at $T = 303$ K and $t_w = 16.5$ h. Circles: experimental data [16]. Solid line: prediction of the model with $\alpha_0 = 2.24$, $\Gamma_0 = 0.23 \text{ s}^{-1}$ and $G_0 = 1.0176$ GPa

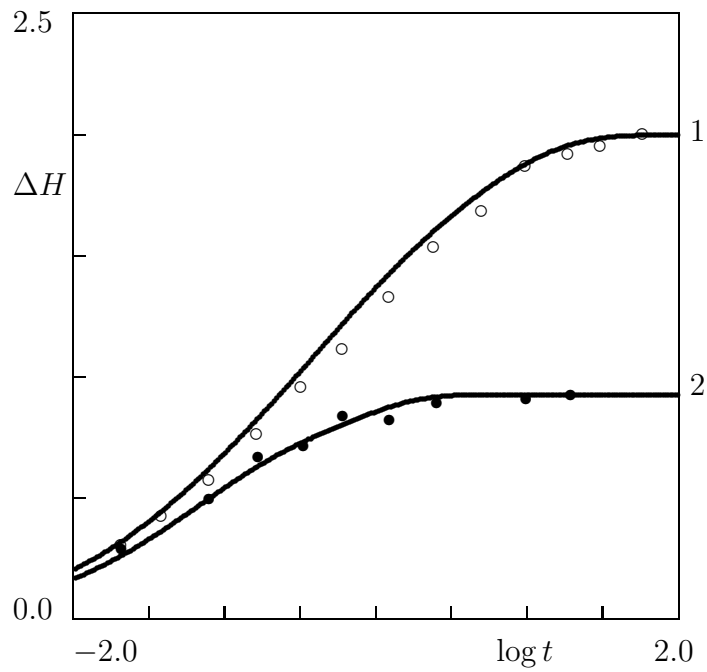


Figure 1:

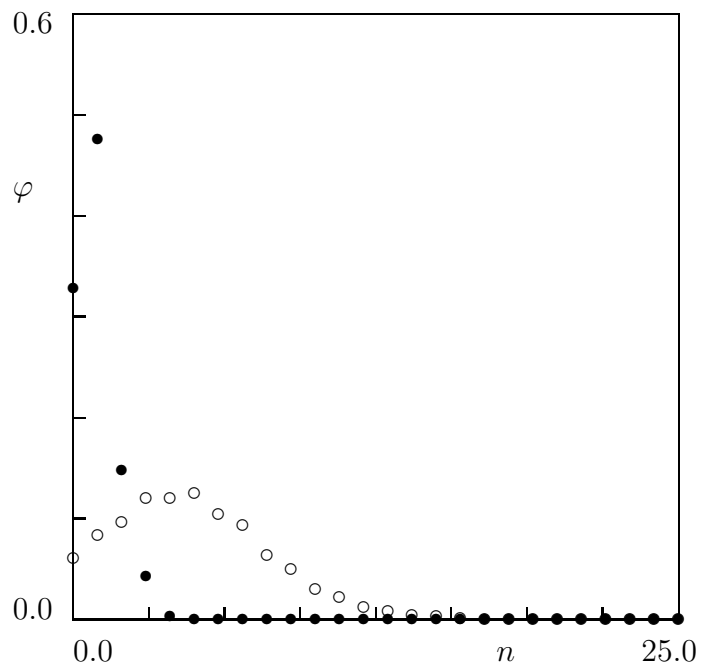


Figure 2:

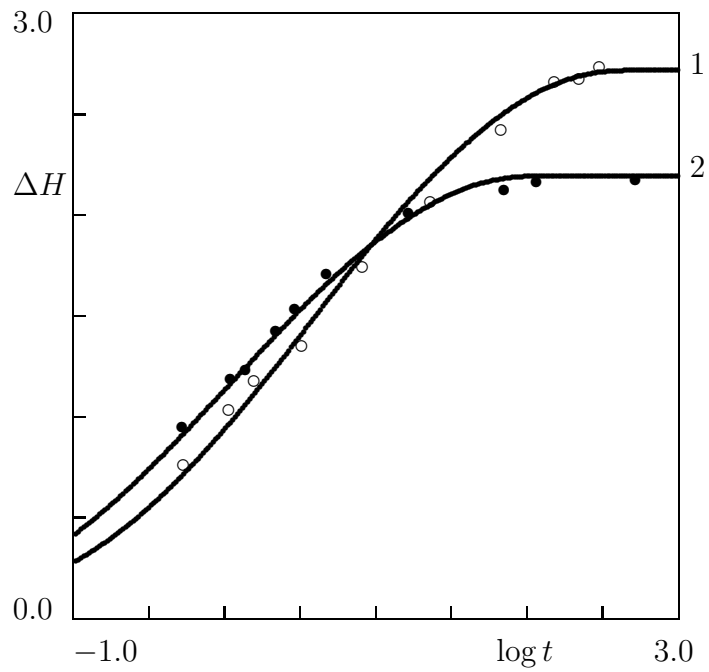


Figure 3:

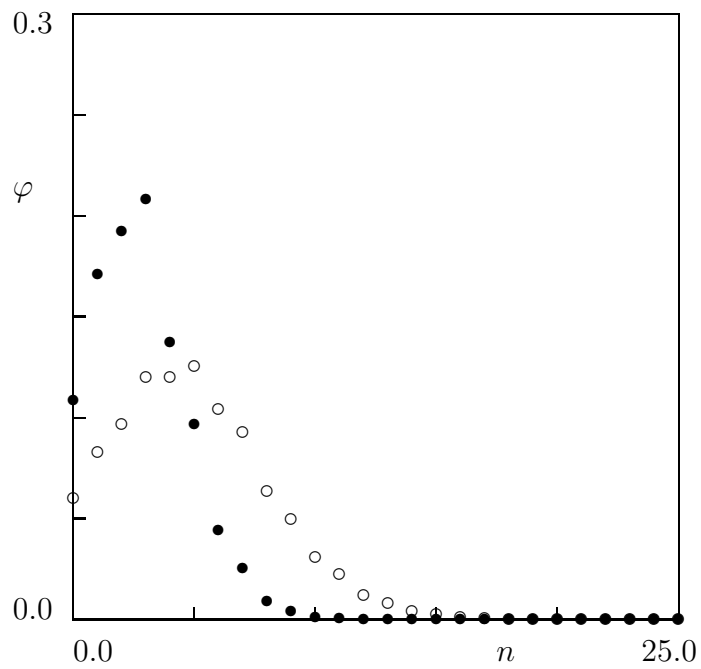


Figure 4:

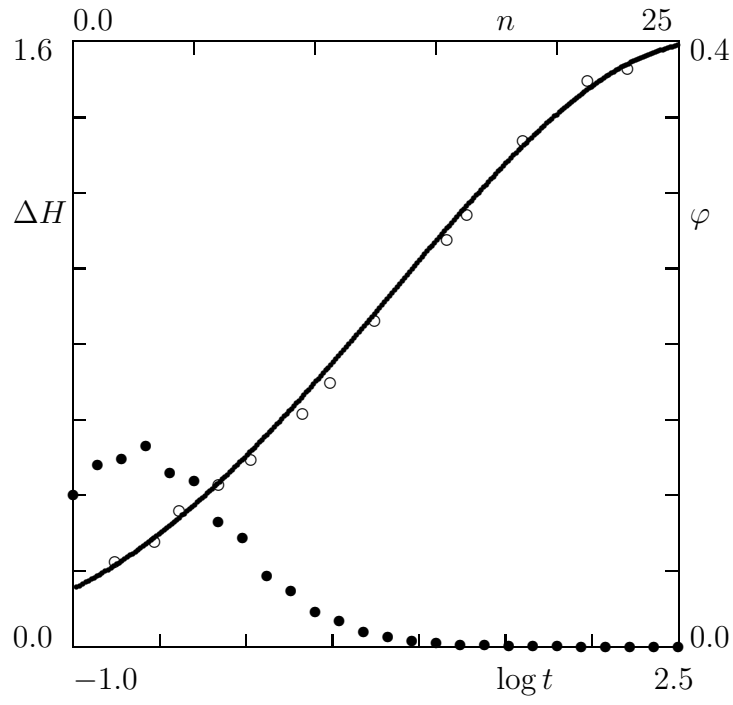


Figure 5:

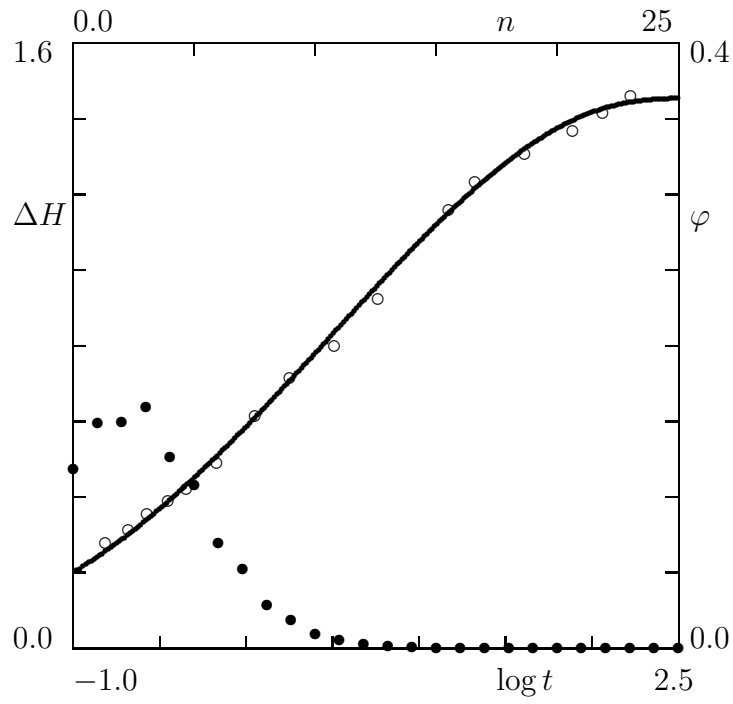


Figure 6:

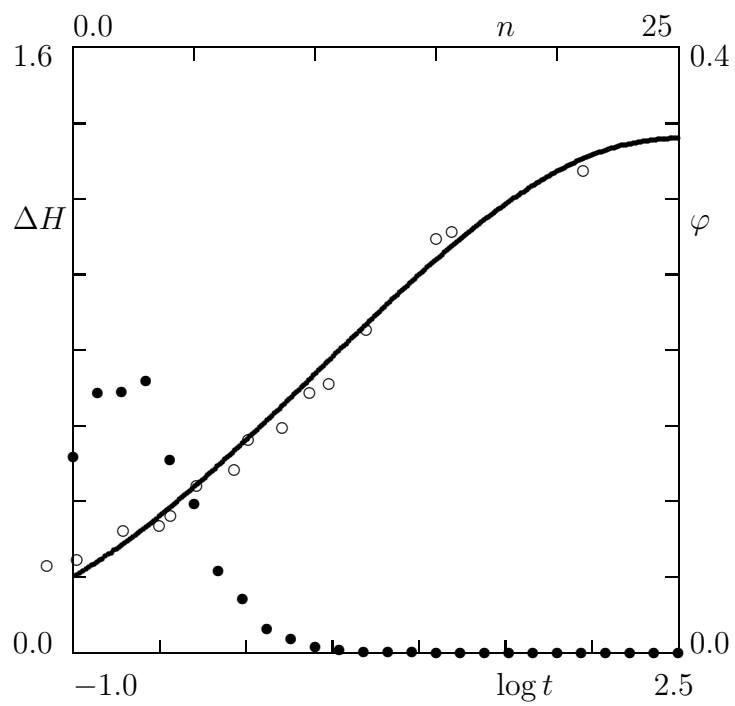


Figure 7:

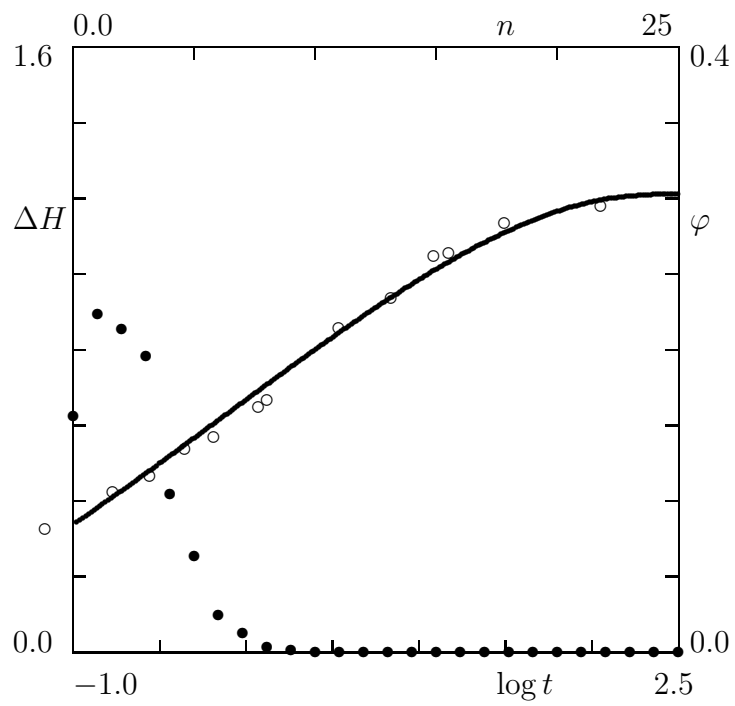


Figure 8:

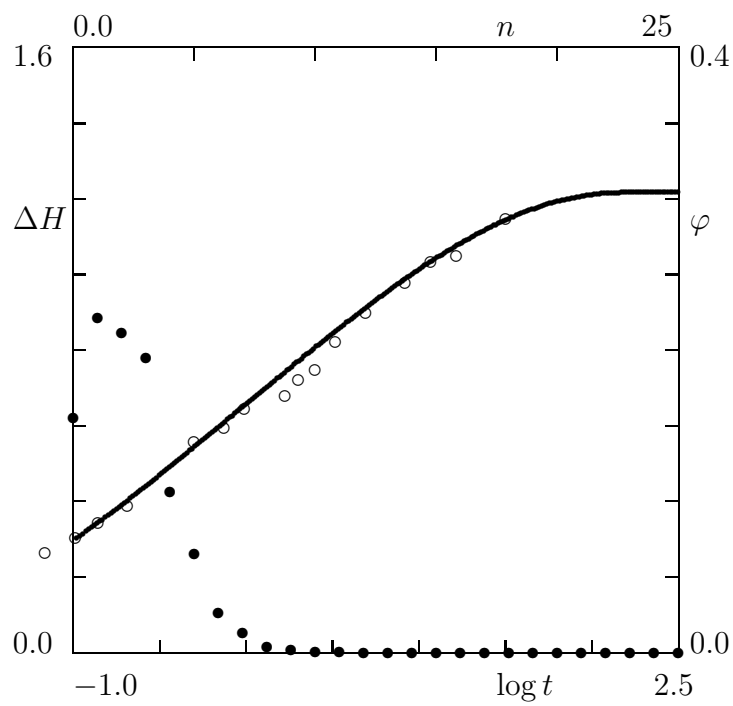


Figure 9:

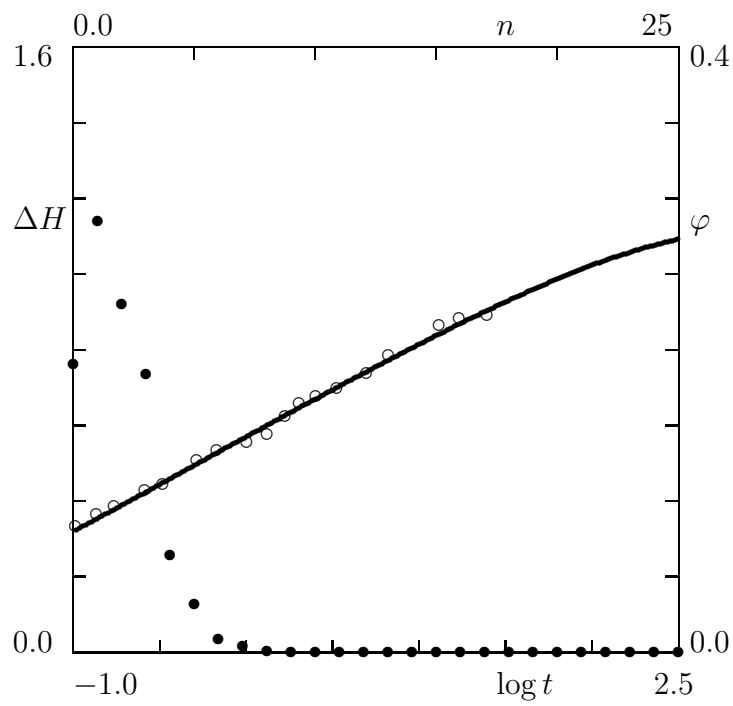


Figure 10:

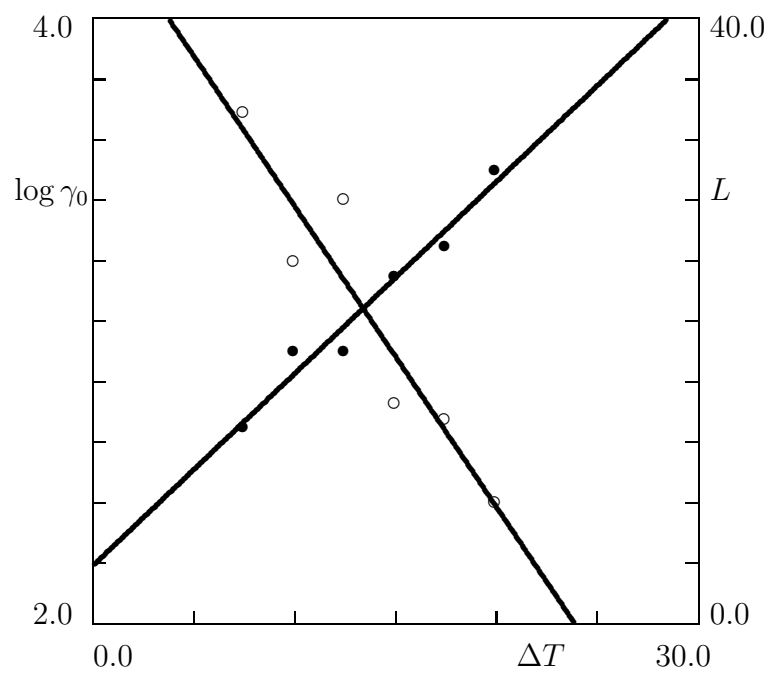


Figure 11:

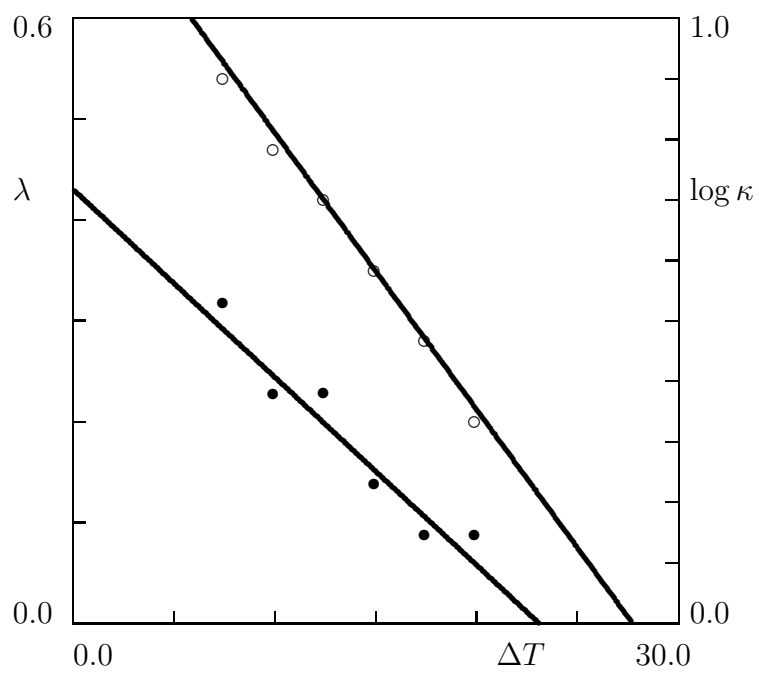


Figure 12:

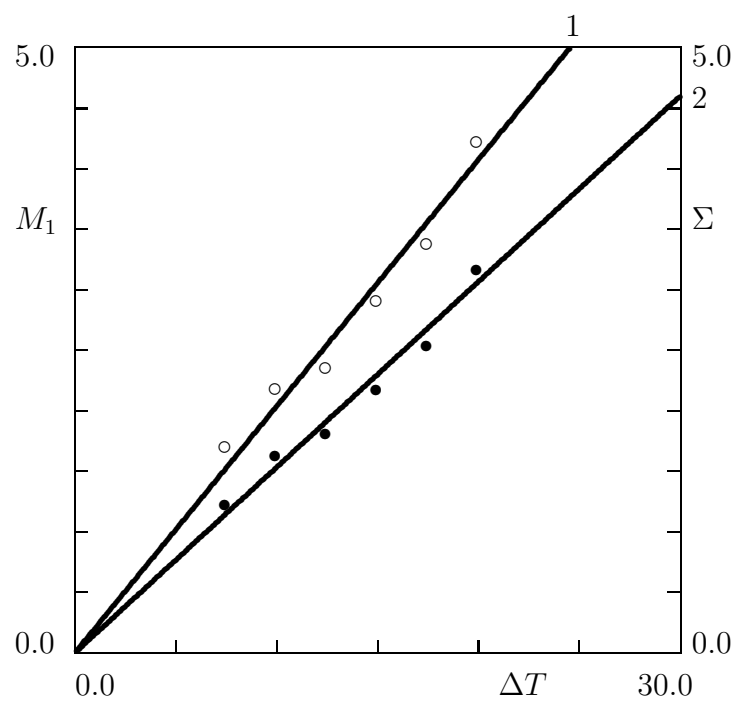


Figure 13:

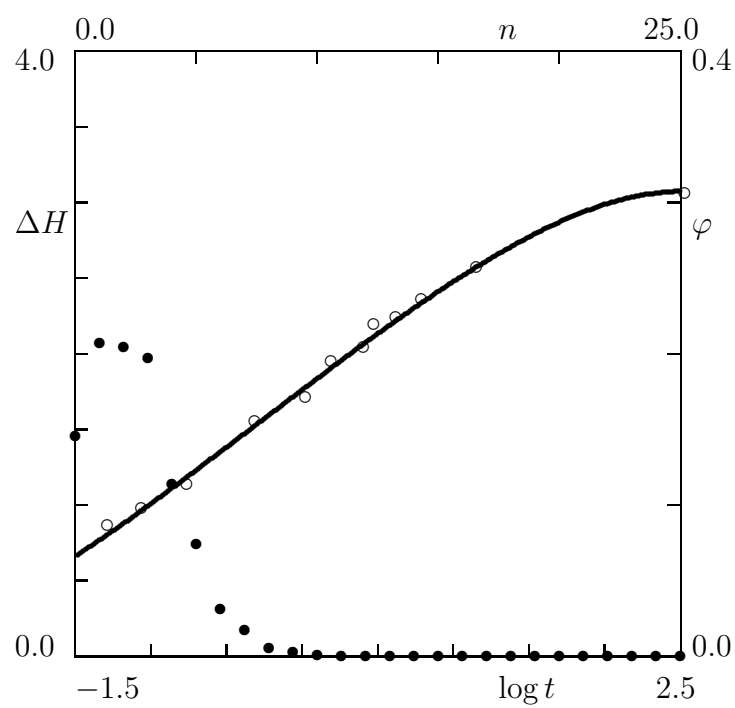


Figure 14:

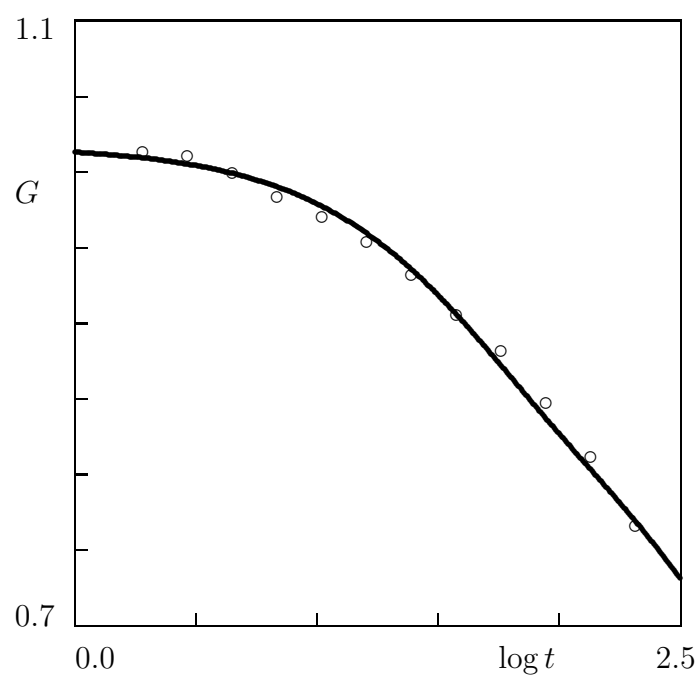


Figure 15: